J. Plasma Phys. (2024), *vol*. 90, 155900301
Published by Cambridge University Press
doi:10.1017/S0022377824000278

Overview of neutral beam injectors for plasma heating and diagnostics developed at Budker INP

Igor Shikhovtsev[1],†, Alexander Ivanov[1], Vladimir Davydenko[1], Yuri Belchenko[1], Grigoriy Abdrashitov[1], Viktor Belov[1], Timur Akhmetov[1], Vladislav Amirov[1], Alexander Brul[1], Peter Deichuli[1], Nikita Deichuli[1], Alexander Donin[1], Alexander Dranichnikov[1], Roman Finashin[1], Daniil Gavrisenko[1], Alexander Gorbovsky[1], Valerian Kapitonov[1], Vyacheslav Kolmogorov[1], Alexey Kondakov[1], Ivan Maslakov[1], Vladimir Oreshonok[1], Vladimir Rashchenko[1], Andrey Sanin[1], Alexey Sorokin[1], Oleg Sotnikov[1], Nikolay Stupishin[1], Roman Vakhrushev[1] and Vadim Vointsev[1]

[1]Budker Institute of Nuclear Physics, Novosibirsk, Russia

(Received 30 October 2023; revised 16 February 2024; accepted 16 February 2024)

An overview of the neutral beam injectors developed at the Budker Institute of Nuclear Physics in Novosibirsk during the last 10 years is presented. These neutral injectors are used for plasma diagnostics, heating and current drive in modern fusion devices with magnetic confinement. An arc or a radio-frequency (RF) discharge generates a plasma in the ion sources of the injectors, and a positive hydrogen or deuterium ion beam is extracted and accelerated by a multiaperture ion-optical system (IOS). The accelerated ion beam is converted into a neutral one in a gas target. The precision multiaperture IOS with spherically concave electrodes provides ballistic focusing of the neutral beam. The high-energy, high-power beam injector based on negative ions, which is currently under development, is described as well. It comprises a RF negative ion source and a wide-aperture electrostatic accelerator separated from the source by a low-energy beam transport line, thereby improving the injector reliability.

Keywords: intense particle beams

1. Introduction

Neutral beams are widely used in the experimental magnetic fusion devices (Hemsworth & Inoue 2005; Takeiri *et al.* 2010; Hopf *et al.* 2021). Over the last three decades the Budker Institute of Nuclear Physics (BINP) has developed and produced neutral beam injectors for plasma diagnostics, auxiliary heating, plasma rotation and current drive for medium-size tokamaks, mirror machines, field-reversed configurations and other magnetic fusion devices in the research centres of Russia, Europe and the USA (Belchenko *et al.* 2018).

† Email address for correspondence: i.v.shikhovtsev@inp.nsk.su

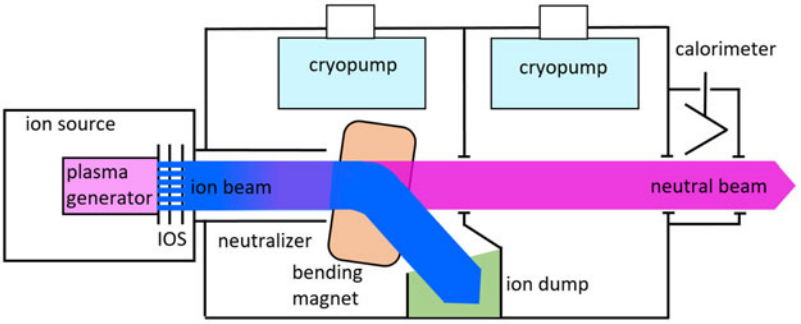

FIGURE 1. Schematic of a neutral beam injector.

Charge-exchange injectors are based on acceleration of positive hydrogen (or deuterium) ions with subsequent neutralization in a gas target. The injectors of this type developed at BINP produce neutral beams with energy from 8 to 80 keV; the beam power ranges from hundreds of kilowatts for diagnostic beams to several megawatts for heating beams. The diagnostic injectors produce focused neutral beams with very small angular divergence of elementary beamlets, high atomic flux at the focal spot, and time modulation. The high-power injectors (up to 2 MW) producing focused beams with small width in the focal region are used for plasma heating in devices with narrow ports or for injection into a desired plasma region.

A typical injector scheme is shown in figure 1. Its main components are an ion source, ion beam accelerator, beam neutralizer and a separator of residual ions with a beam dump (Brown 2004). The ion source includes a plasma chamber, where a hydrogen or deuterium plasma is produced, and a multiaperture ion-optical system (IOS), which extracts and forms an ion beam. The extracted beam has different species, including the molecular ones. After neutralization of the accelerated molecular ions, species with full, one-half and one-third energy are formed. A bending magnet deflects the residual ions into the ion dump. The neutral beam is transported along a beam duct and finally passes through a port in a vacuum vessel of a plasma device towards the confined plasma. The injector has a high-speed pumping system. The beam dump is equipped with an array of thermocouples used for conditioning of the ion source and measuring the parameters of the beam.

Plasma is created using a radio-frequency (RF) or an arc discharge. Most BINP injectors use cold cathode arc discharge through a washer stack channel with subsequent plasma expansion in a chamber surrounded by a multipole magnetic field. This discharge produces a plasma with high proton content and good spatial homogeneity. High thermal loads and erosion of the arc channel imply that the arc generators are mainly used in injectors with a short active pulse (max 1 s). In the RF discharge, on the other hand, erosion of the discharge chamber is negligible, therefore the RF emitter can operate without maintenance in injectors with multisecond pulse lengths. The disadvantage for the diagnostic injectors is that the content of the beam fraction with the total energy is 20 % smaller than from the injectors based on arc plasma generators.

The ion source has a three- or four-electrode (or grid) IOS. The first grid (also called a plasma grid) faces the plasma, the second grid extracts the ions from the plasma, the third grid accelerates the ions and the fourth grid is grounded. To suppress electron backstreaming, the acceleration grid is biased negatively with respect to ground. The ion sources for the diagnostic injectors have four grids, which allows formation of the beams with very small angular divergence. The three-grid systems (without the extraction grid)

https://doi.org/10.1017/S0022377824000278 Published online by Cambridge University Press

are mainly used in the ion sources for heating injectors with a higher initial ion current density of the extracted beams.

Finite ion temperature in the plasma source results in inherent angular divergence of elementary beamlets formed in the apertures of the grids. The beamlet current density at the grid surface is assumed to depend on the angle θ from the beamlet axis as $\exp(-\theta^2/\theta_0^2)$, where θ_0 is the divergence. For a long slit aperture, the divergence in the direction along the slit is determined by the ion temperature. The divergence in the direction across the slits is always larger due to aberrations in the extraction system. Individual beamlets from the grids are directed to one point and merge there, which is called focusing (Brown 2004).

The neutralization efficiency of positive ions in a gas target decreases rapidly with ion energy, so in a positive ion-based injector the injection energy is limited to approximately 120 keV. Such beam energies are sufficient for most existing plasma experiments. New fusion devices (ITER and the next generation) with high density and large plasma radius require neutral beams with an increased energy of 0.5–1 MeV. The neutralization efficiency of negative ions in this energy range is approximately 60 % (Hemsworth & Inoue 2005), so the new generation of high-energy neutral injectors based on neutralization of accelerated negative ions (H^-/D^-) is under development for large tokamaks and stellarators (Speth *et al.* 2006; Takeiri *et al.* 2010; Heinemann *et al.* 2017; Hemsworth *et al.* 2017; Singh *et al.* 2017; Hiratsuka *et al.* 2020; Inoue 2023). Most of the powerful high-energy neutral injectors for fusion devices use the surface plasma method of negative hydrogen ion production, which was discovered and developed at BINP (Belchenko, Dimov & Dudnikov 1974). At present a prototype of a powerful high-energy neutral beam injector is under development at the BINP (Sotnikov *et al.* 2021). An RF surface-plasma source produces a negative ion beam by conversion of the hydrogen plasma atoms on a caesium-coated plasma grid. The specific features include a low-energy ion transport path, energy enhancement using a single-aperture accelerating tube, and a plasma neutralizer. At present the experiments are underway to increase the beam energy to 500 keV with a current of 1.5 A and operation in a multisecond mode up to 100 s. Several improved versions of the RF plasma drivers were tested to increase the pulse length (Gavrisenko *et al.* 2023). The paper gives an overview of these and other studies devoted to the development of neutral beam injectors in recent years.

2. Neutral injectors for plasma diagnostics

The BINP has approximately 50 years of experience in developing the neutral beam injectors for plasma diagnostics (Belchenko *et al.* 2018). A diagnostic neutral beam has energy in the range from 20 to 60 keV, equivalent beam current of 1–10 A and pulse length from 5 ms to 10 s. The beam is extracted from an RF or an arc-discharge plasma emitter and accelerated to the desired energy by a four-grid IOS. Relatively low emission current density of 110–130 mA cm^{-2} allows formation of a beam with the initial angular divergence as small as 10 mrad. A spherical shape of the multiaperture grids provides ballistic focusing of the beam resulting in small dimensions of the focal spot of the diagnostic neutral beam in a plasma. In recent decades the BINP team has developed diagnostic injectors for various plasma devices, for example: the Wendelstein 7-X stellarator at IPP, Greifswald, Germany (Davydenko *et al.* 2016); the C-2W facility at TAE, USA; the T-15MD tokamak at the Kurchatov Institute, Moscow, Russia (Stupishin *et al.* 2016); the ST40 tokamak at Tokamak Energy Ltd, Abingdon, UK. The main parameters of these injectors are listed in table 1.

The injector for charge exchange recombination spectroscopy of impurity atoms and diagnostics of charge exchange neutrals in the Wendelstein 7-X stellarator was designed

https://doi.org/10.1017/S0022377824000278 Published online by Cambridge University Press

Plasma device	W7-X	C-2W	ST40	T-15MD
Diagnostics	CXNPA, CXRS	CXRS	CXRS	CXRS
Isotope	H	H(D)	H	H
Type of plasma emitter	RF	Arc	Arc	Arc
Beam energy, keV	60	44	50	60
Ion beam current, A	8	15.5	3	6.1
Neutral beam current (eq.), A	2.4	9.6	1.4	2.6
Pulse duration, s	10 (2.5 s ON)	0.03	2 (1 s ON)	10 (1 s ON)
Beam modulation	up to 100 Hz	up to 10 kHz	up to 100 Hz	up to 100 Hz
Beam angular divergence, mrad	12	12	10	10
IOS focal distance, m	6	3	4	4
Full energy fraction, %	55	85	>80	84
IOS diameter, mm	205	180	87	160
Plasma grid apertures	∅4 mm × 1057	∅4 mm × 943	4 mm slits	∅4 mm × 745
Year of start operation	2013	2019	2020	2023[a]

[a]The injector is scheduled for connection to the tokamak in 2024.

TABLE 1. Diagnostic injectors developed by BINP in recent years.

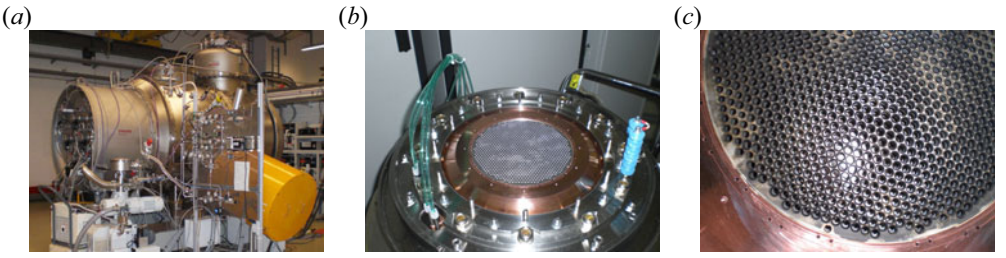

FIGURE 2. (*a*) Diagnostic injector for W7-X stellarator at test stand. (*b*,*c*) View of the plasma grid of the IOS.

to operate under strict conditions of the radiation environment of a large fusion device. Its vacuum tank was made of the non-magnetic and low-cobalt special ASTM/AISI 316 LN (1.4429) stainless steel ($\mu < 1.02$, Co < 500 ppm). The neutral beam had to pass through a long port surrounded by a cryostat. Thus, the IOS was designed to have a large focal length of 6 m. Power supply systems were located in a radiation-protected room and the cable route was approximately 70 m long. The injector is presently located at a test stand (figure 2*a*) in Greifswald. The ion source (yellow) is tilted at an angle of 18°. The chamber is pumped down by two closed cycle Leybold COOLVAC cryopumps with pumping speeds of 60 000 l s^{-1} and 30 000 l s^{-1}. A view of the molybdenum plasma grid of the four-electrode IOS with peripheral cooling is shown in figures 2(*b*) and 2(*c*). The accumulated beam-on time in the modulated regime is limited to 2.5 s for a 10 s pulse length, because the grids are cooled only at the periphery, and because the protective shield of the RF ion source is cooled by a single channel at one end. The design of the plasma chamber is similar to that of the heating injector (Sorokin *et al.* 2010). An RF generator based on a radio tube operates at a rated power of 25 kW and a frequency of 4 MHz.

The diagnostic beam injector for the C-2W facility (TAE, USA) forms a beam with an energy of 44 keV. High beam energy was chosen to ensure low beam attenuation in the

https://doi.org/10.1017/S0022377824000278 Published online by Cambridge University Press

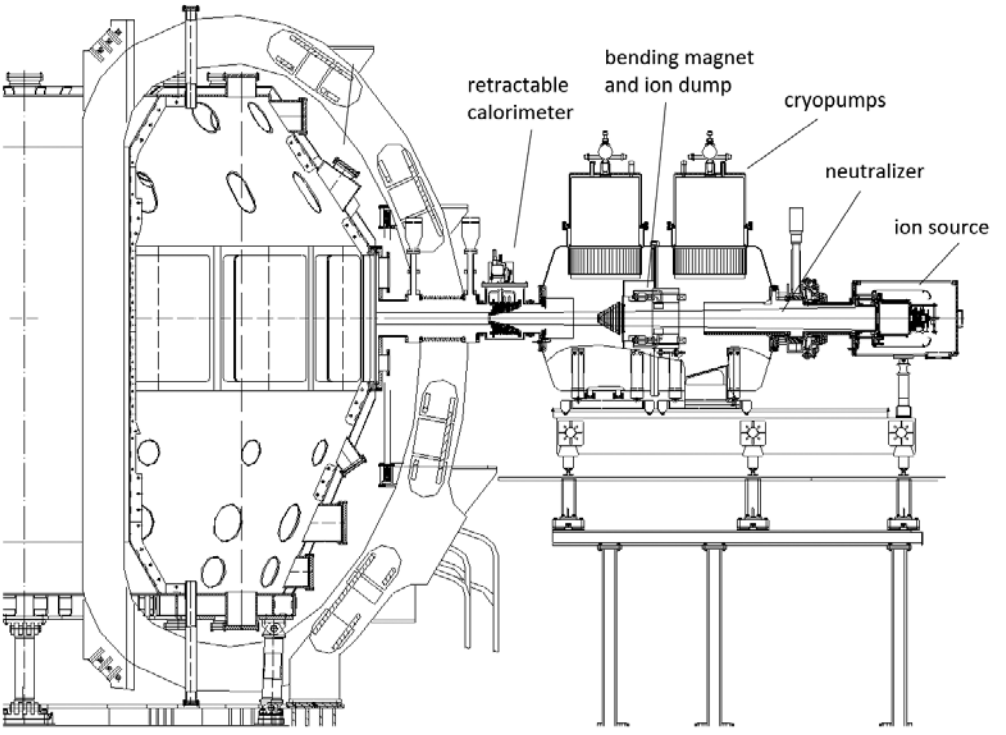

FIGURE 3. Cross-section of the T15-MD tokamak with the diagnostic neutral beam injector connected to the port.

plasma and to allow charge exchange recombination spectroscopy throughout the plasma column to measure the local ion temperature and the velocity of impurity ions (Nations *et al.* 2021) and of the main deuterium ion component (Gupta *et al.* 2021). The ion source is based on an arc plasma generator and its four-electrode IOS is made of chromium zirconium brass. This arc plasma generator is analogous to the one used for the C-2W heating beams and described in detail in Deichuli *et al.* (2015). The injector operates with fast 100 % beam modulation with a frequency of up to 1 kHz. Modulation is carried out by completely turning on/off a high-voltage power supply. For higher frequency up to 10 kHz the beam modulation is performed by rapidly reconnecting the arc discharge current in the plasma source from the anode to the plasma chamber. It changes the plasma generation and the extracted ion current density as well. The beam density modulation depth reaches $\approx$60 %.

The diagnostic injector developed for the T-15MD tokamak forms a hydrogen beam with an energy of 60 keV and an equivalent current of 2.6 A (Stupishin *et al.* 2016). Integrated beam-on time is maximally set to 1 s when the beam is operated in a 10 s pulse with modulation. The diagnostic injector is based on an arc discharge plasma source with a plasma expansion chamber. The spherical shape of the grids and a small angular divergence of 10 mrad provide the relatively small focal spot $\approx$6 cm in diameter in the plasma. The injector was tested at the BINP in 2016 and commissioned at the Kurchatov Institute in 2023. The layout of the injector with the cross-section of the T15-MD tokamak is shown in figure 3.

The diagnostic injector for the ST40 tokamak is the upgraded injector made earlier for the TEXTOR tokamak (Listopad *et al.* 2012). Its plasma source has been replaced by an

https://doi.org/10.1017/S0022377824000278 Published online by Cambridge University Press

Plasma device	C-2U	C-2W	TCV		Globus-M2	ST40	COMPASS
Isotope	H	H	D/H	D/H	D/H	D/H	D
Plasma emitter	Arc	Arc	RF	RF	RF	RF	RF
Beam energy, keV	15	15 → 40	7–28	25–51	50	55/53	80
Ion beam current, A	150	150	up to 55	up to 40	30/36	34/40	20
NB power, MW	1.6	1.7 → 3.5	0.06–1.3	0.24–1.2	1.1/0.9	1.4/1.2	1
Pulse duration, s	0.008	0.03	2	2	1	2	1
Modulation	no	no	yes	yes	yes	yes	yes
Focal distance, m	3.5	3.5	3.8	4.2	3.8	3.4	3.4
Plasma grid apertures	2 mm slits	2 mm slits	3 mm slits	3 mm slits	∅5 mm ×767	∅5 mm ×914	∅6 mm ×502
IOS diameter, cm	34	36	25	25	20	25	21.8
Year	2014	2019	2015	2021	2019	2021	2021

TABLE 2. Parameters of neutral beam injectors for plasma heating.

arc discharge plasma generator with a cold cathode (Stupishin *et al.* 2016), which is more reliable and much easier to operate (although the pulse duration becomes shorter). All power systems were redesigned to work from storages based on supercapacitors due to the absence of a powerful electric network. New supply provides a 2 s injector pulse. A cryogenic system with helium filling has been replaced by an easier-to-operate system with cryocooler heads. A new injector control system uses a hardware platform consisting of an industrial computer with National Instruments modules integrated in LabVIEW.

3. Neutral beam injectors for plasma heating

In recent years the heating neutral beam injectors with a power of approximately 1 MW have been developed and commissioned on tokamaks at SPC, Lausanne, Switzerland (TCV), Ioffe Institute St. Petersburg, Russia (Globus-M2), Tokamak Energy Ltd, England (ST40), IPP, Prague, Czech Republic (COMPASS). The parameters of the injectors are listed in table 2.

The injectors with an increased power and an energy of 15 keV were designed and manufactured in 2014 (Deichuli *et al.* 2015), and the injectors with a tuneable beam energy were made in 2019 (Brul *et al.* 2021). The initial beam energy was set to 15 keV and could be subsequently increased to 40 keV during the beam pulse, so that the fast ion orbits would agree with the controlled external magnetic field ramp-up of the C-2W device (Gota *et al.* 2021). The energy rise time could be varied from 0.2 ms to several milliseconds, and the total pulse length was 30 ms. Thus, the neutral beam power increased from 1.7 MW to 3.5 MW. A particular feature of these injectors was that the ion beam current was kept constant at 150 A during a change in the beam energy. It was achieved by switching the operating mode of the IOS – it worked as a three-electrode system at an energy of 15 keV and was turned to a four-electrode system for an energy of 40 keV.

The heating injector for the Globus-M2 tokamak has a design similar to the injector for C2 (Sorokin *et al.* 2010) with minor changes in the IOS to operate with a deuterium beam at an energy of 50 keV (Shchegolev *et al.* 2023). The first experiments on plasma heating by two neutral beams demonstrated the increase in ion temperature at the plasma axis up to ∼4 keV at the electron density of 5×10^{19} m^{-3} (Kurskiev *et al.* 2023).

Two heating injectors delivering D/H beams with a power of 1 MW each and energies of 25 and 51 keV operate at the TCV tokamak (Karpushov *et al.* 2017, 2023).

https://doi.org/10.1017/S0022377824000278 Published online by Cambridge University Press

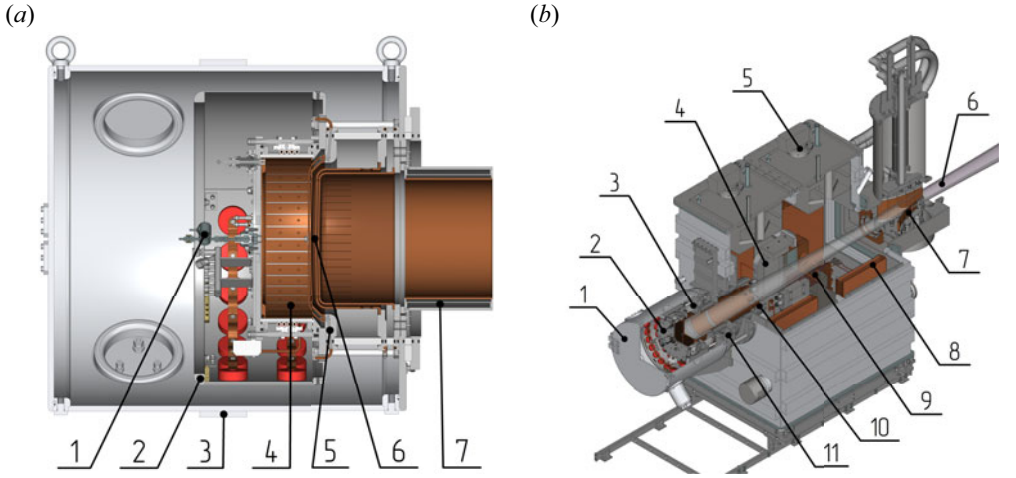

FIGURE 4. (*a*) Layout of the ion source of the second TCV injector: 1, gas puffing valve; 2, inner electrostatic screen; 3, outer magnetic screen; 4, RF plasma box; 5, IOS insulation unit; 6, IOS grids; 7, neutralizer tube. (*b*) Three-dimensional model of the second TCV injector: 1, outer magnetic screen of ion source; 2, RF plasma box; 3, IOS, 4, bending magnet;5, cryocooler head; 6, neutral beam; 7, calorimeter; 8, cryopump panels; 9, ion dump; 10, neutralizer; 11, alignment unit.

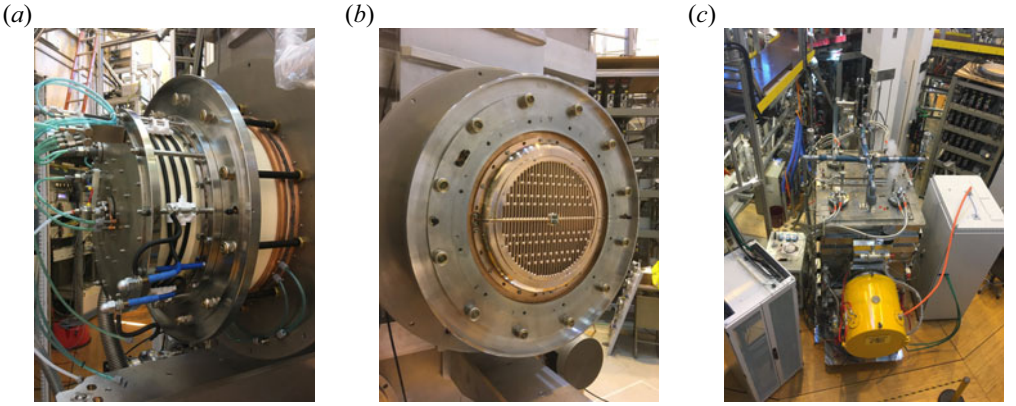

FIGURE 5. (*a*) Ion source, (*b*) plasma grid of the IOS and (*c*) injector at the TCV tokamak.

Radio-frequency generators with power up to 60 kW at a frequency of 4 MHz are used for plasma production in the ion sources. A multiaperture IOS consists of three spherically shaped slitted grids made of chromium zirconium brass. It provides ballistic beam focusing, and produces a sufficiently narrow beam with an angular divergence of 14×5 mrad. The grids are cooled at the periphery, and the plasma grid is additionally cooled in the centre, which allows extension of the beam pulse to 2 s. The injectors are operated in a modulated mode forming the beams with varying energy and power during the pulse according to a preset sequence or using a real-time feedback signal. General views of the second injector and its ion source are shown in figure 4 and in the photographs in figure 5.

The main parameters of the injectors were studied at the BINP test stands and at plasma devices. Beam profiles were measured by a set of secondary emission sensors mounted in the form of a cross at a distance of 3.3 m from the IOS (Sorokin *et al.* 2020). The

https://doi.org/10.1017/S0022377824000278 Published online by Cambridge University Press

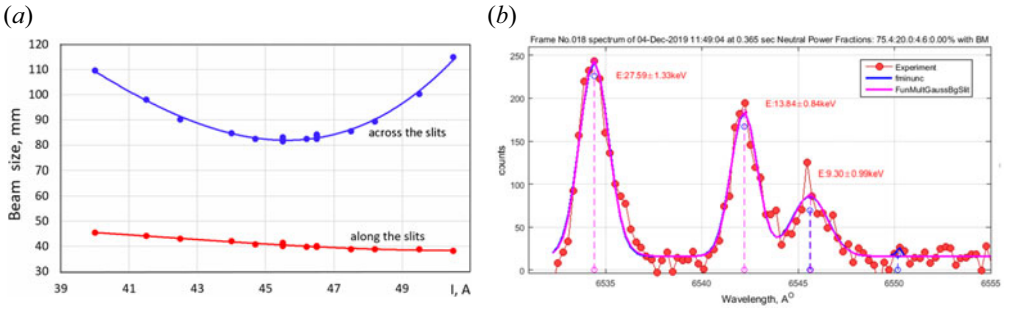

FIGURE 6. (*a*) Change of 27 keV beam sizes across and along the slits versus ion beam current. (*b*) Doppler-shifted spectra of deuterium 27 keV beam of H-α emission line.

widths of the 27 keV beam at the 1/e level in the directions along and across the grid slits versus the ion beam current for the first injector after its upgrade are shown in figure 6(*a*). At the optimal ion beam current minimizing the width across the slits, the dimensions of the neutral beam are 4×8 cm. The molecular fractions of the neutral beam were determined using the Doppler optical emission diagnostics. The Doppler-shifted spectra of the hydrogen emission lines shown in figure 6(*b*) (Tec 2020) illustrate the ratio of the atoms with energies E, $E/2$, $E/3$ in the beam. The neutral beam comprises 75 % atoms with full energy (left-hand peak in figure 6*b*). The beam dimensions were also inferred from measurement of the temperature distribution over the surface of a tungsten tile heated by the beam (Karpushov *et al.* 2023). The local temperature rise was proportional to the local beam power density. The focal length, calculated from measuring the beam profiles at various distances from the IOS, is ≈380/400 cm (across/along the slits). The inherent beamlet divergence angle is defined as a ratio of the beam half-width in the focal plane to the focal length. For the first and the second injectors, the measured divergence was $1.35^\circ/0.57^\circ$ and $0.79^\circ/0.3^\circ$ (across/along the slits).

The BINP heating injector of a deuterium beam with an energy of 55 keV and a power of 1 MW is one of the two injectors on the ST40 tokamak (McNamara *et al.* 2023). An injector tank with a cryogenic pumping system based on the Sumitomo cool heads is the same as for the TCV injectors. A high-voltage power system (manufactured by JEMA) and an RF system are supplied from storages based on supercapacitors. The IOS geometry is different from the one in the injector for the TCV tokamak. The tokamak port is round and large enough with a diameter of 320 mm. The ion source produces a beam with a circular initial cross-section 250 mm in diameter. A set of 5 mm holes fills the emission area of the plasma grid forming a hexagonal structure with a transparency of 32 %. The nominal current density of a beam extracted from an elementary cell is 190 mA cm^{-2}. The measured angular divergence of the beam is 13 mrad.

Two 300 kW, 40 keV heating injectors of deuterium and hydrogen atoms have been operated since 2011 at IPP in Prague (Deichuli *et al.* 2012). The new heating neutral beam was commissioned in 2021 and tested at nominal parameters (80 keV, 1 MW deuterium beam) at the COMPASS tokamak before the shutdown of the latter. This injector is a prototype for the new COMPASS-U tokamak.

4. High energy negative ion-based injector

A high-energy injector based on negative ion acceleration is under development at the BINP (Ivanov *et al.* 2013). It includes several innovative components: a RF negative ion source with thermal stabilization of electrodes and directed deposition of caesium vapour to the plasma electrode (Belchenko *et al.* 2016); a low-energy beam transport (LEBT)

https://doi.org/10.1017/S0022377824000278 Published online by Cambridge University Press

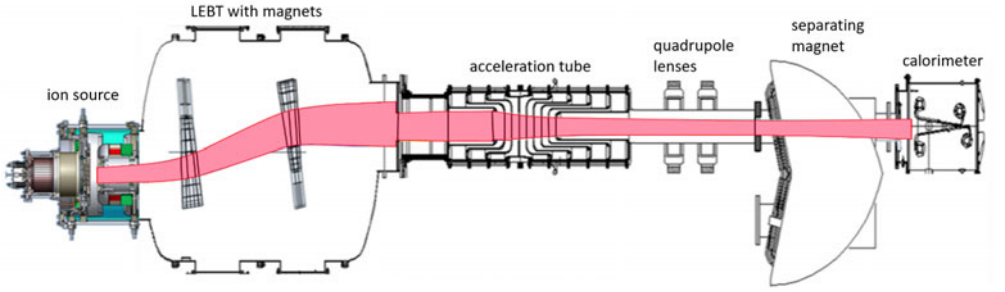

FIGURE 7. High-voltage acceleration test stand. Red lines show calculated ion trajectories for 30 mrad initial divergence and 85 keV energy.

section needed to purify the beam from parasitic particles leaving the ion source and to protect the source from particles backstreaming from the accelerator; an accelerator, separated from the source with LEBT; a plasma neutralizer of accelerated negative ions.

Negative ion beam formation, acceleration and transport are studied at a high-voltage acceleration test stand, schematically shown in figure 7. An intense 120 keV negative ion beam, produced by a surface-plasma negative ion source is directed to the LEBT vacuum tank, equipped with cryopumps and a pair of immersed dipole magnets. The LEBT bending magnets shift the beam axis between the source and the high-voltage accelerator. This beam shift and high pumping speed of the LEBT tank reduce the flux of the accompanying harmful species moving from the source to the acceleration tube and prevents positive ions and neutrals from backstreaming into the ion source. It increases the high-voltage strength of the accelerator. The acceleration tube has a wide aperture, which provides better tube pumping, thus reducing beam losses and production of secondary particles, and increasing the high-voltage strength of the tube. The accelerated beam passes through a high-energy beam transport line (HEBT) with quadrupole lenses towards a calorimeter. A separation magnet is installed before the calorimeter to bend the accelerated beam to the recuperator tube (not shown in figure 7). The trajectories of H^- ions in the LEBT, the acceleration tube and the HEBT calculated by COMSOL are shown in figure 7 by the red lines. Figure 7 demonstrates that ~60 %–70 % of the negative ion beam extracted from the source with an initial divergence of 30 mrad enter the accelerator through a 260 mm diameter input diaphragm, and the acceleration tube provides 100 % beam passage. The beam losses during its transport through the LEBT tank were caused by the beam divergence and by the H^- ion stripping in the vacuum tank. These losses agreed well with the calculations (Sotnikov *et al.* 2021) using the ion optical code IBSimu (Kalvas *et al.* 2010). The accelerated H^- beam is focused by the quadrupole lenses. The profile and intensity of the beam are measured by a calorimeter at a 10 m distance from the ion source.

A schematic diagram of the negative ion source and its photograph are shown in figure 8. The plasma produced in the RF driver (figure 8*b*) flows through an expansion chamber with a multipole magnetic wall confining the plasma towards the plasma grid with the dipole magnetic filter. The dipole field suppresses transverse electron diffusion and decreases the electron temperature and density in the region of negative ion production and extraction close to the plasma grid. The negative ions are generated at the plasma grid surface by conversion of the plasma particles. This surface conversion is significantly enhanced due to caesium coverage of the plasma grid. Caesium is supplied from heated caesium distribution galleries located at the plasma grid periphery (figure 8*c*). The plasma

https://doi.org/10.1017/S0022377824000278 Published online by Cambridge University Press

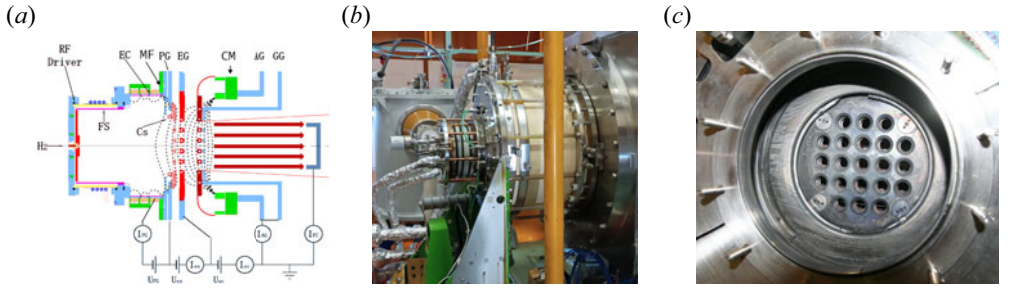

FIGURE 8. (*a*) Schematic of the 1.5 A ion source: Faraday shield (FS); expansion chamber (EC); magnetic filter (MF); plasma grid (PG); caesium (Cs); extraction grid (EG); correction magnet (CM); acceleration grid (AG); ground grid (GG). (*b*) The RF ion source attached to the LEBT tank. (*c*) View from the RF driver side to the surface of plasma grid with 21 emission apertures and two caesium distribution tubes.

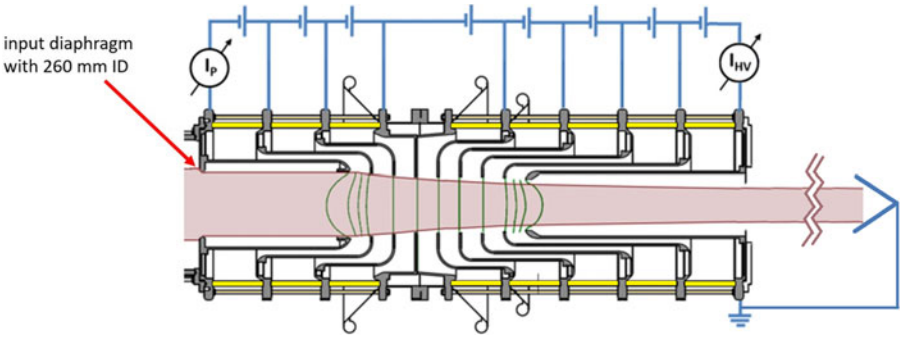

FIGURE 9. Cross-section of the acceleration tube and electrode connections to the power supply. Currents in the electrode circuit are measured by I_P and I_{HV}. Green lines show the calculated equipotential lines for all gaps powered up to 35 kV each. Red lines show the calculated trajectories for the beam with an initial energy of 85 keV and divergence at the source of 30 mrad (Sotnikov *et al.* 2021).

grid is biased positively with respect to the expansion chamber in order to collect the plasma electrons and reduce the flow of electrons extracted together with the negative ions. The acceleration grid is electrically connected to the ground grid, so effectively a three-electrode multiaperture IOS is used for negative ion beam formation. The emission apertures of the plasma grid with the internal diameter of 16 mm and conical chamfers for better extraction of the negative ions are arranged in a rectangular array on the grid surface. Experiments were carried out with 21 open apertures (figure 8*c*).

At the RF power of 37 kW the extracted beam has a current of 1 A and 100 keV energy in a 10 s pulse, and the emission current density is 240–260 A m^{-2}. The prepared upgrade of the RF power supply to 70 kW will allow achieving the design ion beam current of 1.5 A. The RF plasma driver is studied in detail in Gavrisenko *et al.* (2023).

A schematic of the acceleration tube with electric connections and calculated beam trajectories is shown in figure 9. The accelerated beam is compressed by the electrostatic lenses formed in the first accelerating gaps. It is clear that the acceleration tube with the voltage above 35 kV at each gap provides focusing of a 85 keV beam and its full passage through the acceleration tube when the diameter of the input diaphragm is less than 260 mm.

https://doi.org/10.1017/S0022377824000278 Published online by Cambridge University Press

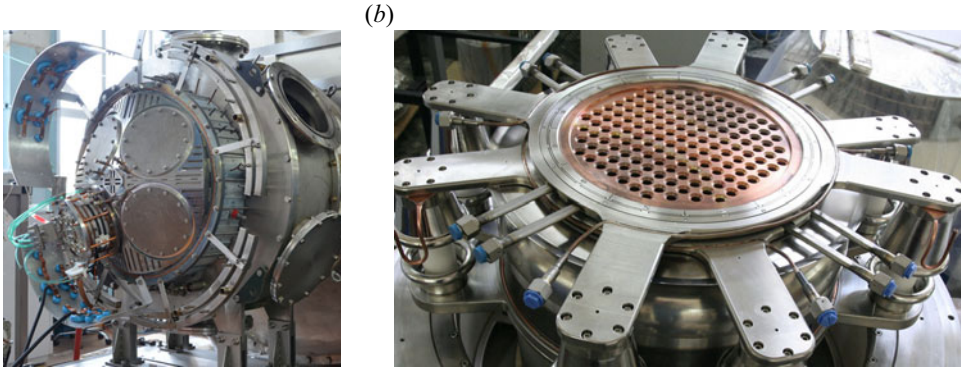

FIGURE 10. (*a*) Photograph of the 9 A ion source attached to the LEBT tank. (*b*) View onto the plasma grid with 145 apertures.

As seen in the high-voltage circuit of figure 9, the total accelerated current I_P is the current flowing from the high-voltage platform, and the current I_{HV} in the circuit of the last high-voltage electrode is the current leaving the acceleration tube. Their difference $I_P - I_{\mathrm{HV}}$ corresponds to the current of charged particles intercepted by the accelerating electrodes. The accelerated current I_P of approximately 0.6 A was achieved in the experiments with the source beam current of 0.86 A, and the voltage of 117 keV. The measured current of intercepted particles in this case was $I_P - I_{\mathrm{HV}} \approx 0.1$ A $\approx 0.16 I_P$. This relatively high value of interception was mainly caused by the low voltage (<35 kV) at each of the first accelerating gaps and by poor alignment of the ion beam with the acceleration tube axis. The 100 % passage of the accelerated beam was demonstrated, when the diameter of the input diaphragm was decreased to 200 mm (Sotnikov *et al.* 2021).

The ion source with a negative ion beam current of 9 A, a beam energy up to 120 keV and a pulse duration up to 100 s was designed and manufactured at BINP (Sotnikov *et al.* 2021). It includes four RF plasma drivers and uses a four-grid IOS with 145 apertures for beam extraction. Additional pumping is provided at the IOS sides. Thermal stabilization of the IOS grids will be provided by circulating a coolant through internal channels. An IOS insulator unit with an expansion chamber and a plasma grid are shown in figures 10(*a*) and 10(*b*), respectively. A four-channel RF power supply system has been manufactured. Installation of the RF drivers and assembly of the high-voltage power supply system will complete the RF system.

5. Conclusion

The BINP has developed and produced more than 50 neutral beam injectors for plasma heating and diagnostics over the last 30 years. The current and future activities are focused on the development of ion sources and injectors with power up to 10 MW and continuous operation. These studies are supported by national scientific programs aimed at constructing new plasma devices and developing innovative plasma technologies (Belchenko *et al.* 2021). The scientific program on creation of a new generation of magnetic mirror devices for plasma confinement is directly related to the BINP (Skovorodin *et al.* 2023).

Acknowledgements

Editor C. Forest thanks the referees for their advice in evaluating this article.

https://doi.org/10.1017/S0022377824000278 Published online by Cambridge University Press

Funding

The work was partially supported by the Ministry of Science and Higher Education of the Russian Federation.

Declaration of interests

The authors report no conflict of interest.

REFERENCES

BELCHENKO, YU., ABDRASHITOV, G., DEICHULI, P., IVANOV, A., GORBOVSKY, A., KONDAKOV, A., SANIN, A., SOTNIKOV, O. & SHIKHOVTSEV, I. 2016 Inductively driven surface-plasma negative ion source for N-NBI use (invited). *Rev. Sci. Instrum*. **87** (2), 02B316.

BELCHENKO, YU.I., *et al.* 2018 Studies of ion and neutral beam physics and technology at the Budker Institute of Nuclear Physics, SB RAS. *Phys. Usp*. **61** (6), 531–581.

BELCHENKO, YU.I., BURDAKOV, A.V., DAVYDENKO, V.I., GORBOVSKII, A.I., EMELEV, I.S., IVANOV, A.A., SANIN, A.L. & SOTNIKOV, O.Z. 2021 Possible scheme of atomic beam injector for plasma heating and current drive at the TRT tokamak. *Plasma Phys. Rep*. **47** (11), 1151–1157.

BELCHENKO, YU.I., DIMOV, G.I. & DUDNIKOV, V.G. 1974 A powerful injector of neutrals with a surface-plasma source of negative ions. *Nucl. Fusion* **14** (1), 113–114.

BROWN, I.G. (Ed.) 2004 *The Physics and Technology of Ion Sources*, 2nd edn. Wiley-VCH.

BRUL, A.V., *et al.* 2021 High-power neutral beam injector with tunable beam energy for plasma heating and stabilization. *Plasma Phys. Rep*. **47** (6), 518–525.

DAVYDENKO, V., DEICHULI, P., IVANOV, A., STUPISHIN, N., KAPITONOV, V., KOLMOGOROV, A., IVANOV, I., SOROKIN, A. & SHIKHOVTSEV, I. 2016 Recent progress in development of neutral beams for fusion studies. *AIP Conf. Proc*. **1771** (1), 030025.

DEICHULI, P., *et al.* 2012 Commissioning of heating neutral beams for COMPASS-D tokamak. *Rev. Sci. Instrum*. **83** (2), 02B114.

DEICHULI, P., DAVYDENKO, V., IVANOV, A., KOREPANOV, S., MISHAGIN, V., SMIRNOV, A., SOROKIN, A. & STUPISHIN, N. 2015 Low energy, high power hydrogen neutral beam for plasma heating. *Rev. Sci. Instrum*. **86** (11), 113509.

GAVRISENKO, D.YU., SHIKHOVTSEV, I.V., BELCHENKO, YU.I., GORBOVSKIY, A.I., KONDAKOV, A.A., SOTNIKOV, O.Z., SANIN, A.L., VOINTSEV, V.A. & FINASHIN, R.A. 2023 Comparative analysis of high-frequency plasma drivers with various protective screens for atomic injectors with multi-second pulse duration. *Plasma Phys. Rep*. **49** (10), 1169–1179.

GOTA, H., *et al.* 2021 Overview of C-2W: high temperature, steady-state beam-driven field-reversed configuration plasmas. *Nucl. Fusion* **61** (10), 106039.

GUPTA, D.K., NATIONS, M., SWEENEY, J., AVILES, J., LEINWEBER, H. & MARSHALL, R.S. 2021 Main ion charge exchange recombination spectroscopy on C-2W FRC plasmas. *Rev. Sci. Instrum*. **92** (7), 073508.

HEINEMANN, B., FANTZ, U., KRAUS, W., SCHIESKO, L., WIMMER, C., WÜNDERLICH, D., BONOMO, F., FRÖSCHLE, M., NOCENTINI, R. & RIEDL, R. 2017 Towards large and powerful radio frequency driven negative ion sources for fusion. *New J. Phys*. **19** (1), 015001.

HEMSWORTH, R.S. & INOUE, T. 2005 Positive and negative ion sources for magnetic fusion. *IEEE Trans. Plasma Sci*. **33** (6), 1799–1813.

HEMSWORTH, R.S., *et al.* 2017 Overview of the design of the ITER heating neutral beam injectors. *New J. Phys*. **19** (2), 025005.

HIRATSUKA, J., KASHIWAGI, M., ICHIKAWA, M., UMEDA, N., SAQUILAYAN, G.Q., TOBARI, H., WATANABE, K., KOJIMA, A. & YOSHIDA, M. 2020 Achievement of high power and long pulse negative ion beam acceleration for JT-60SA NBI. *Rev. Sci. Instrum*. **91** (2), 023506.

HOPF, C., STARNELLA, G., DEN HARDER, N. & FANTZ, U. 2021 Neutral beam injection for fusion reactors: technological constraints versus functional requirements. *Nucl. Fusion* **61** (10), 106032.

INOUE, T. 2023 *Development of High-Current Negative-Ion-Based Beam Source at the National Institutes for Quantum Science and Technology (QST) in Japan for JT-60 U and ITER Neutral Beam*

Injectors. Springer Series on Atomic, Optical, and Plasma Physics, vol. 124, pp. 577–607. Springer International Publishing.

IVANOV, A.A., *et al.* 2013 Development of a negative ion-based neutral beam injector in Novosibirsk. *Rev. Sci. Instrum.* **85** (2), 02B102.

KALVAS, T., TARVAINEN, O., ROPPONEN, T., STECZKIEWICZ, O., ÄRJE, J. & CLARK, H. 2010 IBSIMU: a three-dimensional simulation software for charged particle optics. *Rev. Sci. Instrum.* **81** (2), 02B703.

KARPUSHOV, A.N., *et al.* 2017 Neutral beam heating on the TCV tokamak. *Fusion Engng Des.* **123**, 468–472.

KARPUSHOV, A.N., *et al.* 2023 Upgrade of the neutral beam heating system on the TCV tokamak — second high energy neutral beam. *Fusion Eng. Des.* **187**, 113384.

KURSKIEV, G.S., *et al.* 2023 Hot ion mode in the Globus-M2 spherical tokamak. *Plasma Phys. Rep.* **49** (4), 403–418.

LISTOPAD, A., COENEN, J., DAVYDENKO, V., IVANOV, A., MISHAGIN, V., SAVKIN, V., SCHWEER, B., SHULZHENKO, G. & UHLEMANN, R. 2012 Use of the focusing multi-slit ion optical system at RUssian Diagnostic Injector (RUDI). *Rev. Sci. Instrum.* **83** (2), 02B707.

MCNAMARA, S.A.M., *et al.* 2023 Achievement of ion temperatures in excess of 100 million degrees Kelvin in the compact high-field spherical tokamak ST40. *Nucl. Fusion* **63** (5), 054002.

NATIONS, M., GUPTA, D., SWEENEY, J., FRAUSTO, L. & TOBIN, M. 2021 Measurements of impurity ion temperature and velocity distributions via active charge-exchange recombination spectroscopy in C-2W. *Rev. Sci. Instrum.* **92** (5), 053512.

SHCHEGOLEV, P.B., *et al.* 2023 Neutral injection complex for Globus-M2 spherical tokamak. *Plasma Phys. Rep.* **49** (12), 1501–1514.

SINGH, M.J., BOILSON, D., POLEVOI, A.R., OIKAWA, T. & MITTEAU, R. 2017 Heating neutral beams for ITER: negative ion sources to tune fusion plasmas. *New J. Phys.* **19** (5), 055004.

SKOVORODIN, D.I., *et al.* 2023 Gas-dynamic multiple-mirror trap GDMT. *Plasma Phys. Rep.* **49** (9), 1039–1086.

SOROKIN, A., BELOV, V., DAVYDENKO, V., DEICHULI, P., IVANOV, A., PODYMINOGIN, A., SHIKHOVTSEV, I., SHULZHENKO, G., STUPISHIN, N. & TIUNOV, M. 2010 Characterization of 1 MW, 40 keV, 1 s neutral beam for plasma heating. *Rev. Sci. Instrum.* **81** (2), 02B108.

SOROKIN, A.V., AKHMETOV, T.D., BRUL, A.V., DAVYDENKO, V.I., IVANOV, A.A., KARPUSHOV, A.N., MISHAGIN, V.V. & SHIKHOVTSEV, I.V. 2020 Update of ion-optical system of neutral beam of tokamak à configuration variable. *Rev. Sci. Instrum.* **91** (1), 013323.

SOTNIKOV, O., *et al.* 2021 Development of high-voltage negative ion based neutral beam injector for fusion devices. *Nucl. Fusion* **61** (11), 116017.

SPETH, E., *et al.* 2006 Overview of the RF source development programme at IPP garching. *Nucl. Fusion* **46** (6), S220–S238.

STUPISHIN, N.V., *et al.* 2016 Multi-second neutral beam injector (60 kV, 6 A) for plasma diagnostics in the upgraded T-15 device. *AIP Conf. Proc.* **1771** (1), 050012.

TAKEIRI, Y., *et al.* 2010 High performance of neutral beam injectors for extension of LHD operational regime. *Fusion Sci. Technol.* **58** (1), 482–488.

TEC 2020 Technical manual for heating neutral beam injector for the TCV tokamak.